Contribution from the Department of Chemistry,
University of Wisconsin, Madison, Wisconsin 53706

# Bonding in Ring Whizzers. I. Photoelectron Spectra and Molecular Orbital Calculations for $(\eta^5\text{-}C_6H_7)Mn(CO)_3$, $(\eta^5\text{-}C_7H_9)Mn(CO)_3$, and $(\eta^5\text{-}C_7H_7)Mn(CO)_3$

THOMAS H. WHITESIDES,* DENNIS L. LICHTENBERGER, and RICHARD A. BUDNIK

*Received July 10, 1974*

AIC40457W

A series of calculations, checked by reference to photoelectron spectral (PES) data, is used to interpret the electronic structure and elucidate the principal bonding interactions in a series of cyclic pentadienylmanganese tricarbonyl complexes. A linear correlation is obtained between the calculated eigenvalues and the observed ionization potentials. This correlation suggests that deviations from Koopman's theorem are reasonably constant in these complexes and that the PES data can be adequately assigned by the results of the calculations. Two important conclusions result from this study. (1) The principal bonding interaction between the organic ligand and the metal is due to the interaction of the a'(e$_1$'') level of the pentadienyl moiety with the metal $d_{xz}$ orbital; this interaction is considerably more important than the a''(e$_1$'')–$d_{yz}$ interaction. (2) Calculations indicate a low-lying virtual level in $C_7H_7Mn(CO)_3$, resulting from the interaction of the $\pi^*$ level with a''(e$_2$'') which may play an important role in the fluxional degenerate rearrangement of this molecule.

## Introduction

Because of our interest in molecules known as "ring whizzers,"[1] we have undertaken a detailed investigation of the bonding in $\eta^4$-diene and $\eta^5$-dienyl complexes, with the eventual aim of understanding the stereoelectronic nature of the fluxional process. Since our prior contribution to this area had been the synthesis and characterization of the fluxional behavior of $\eta^5$-cycloheptatrienylmanganese tricarbonyl (**4**),[3] we initiated our program with the investigation of this molecule and of the related $\eta^5$ manganese species **2** and **3**.

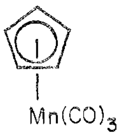

**1**

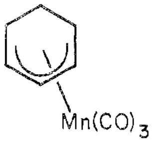

**2**

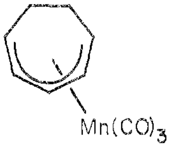

**3**

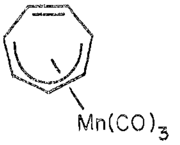

**4**

The study of this series of molecules was aided by several circumstances. First, other groups in these laboratories have developed a reasonably economical method for carrying out approximate molecular orbital calculations on transition metal compounds of this complexity. Second, the molecules in question are stable and well characterized, to the extent that high-quality crystal structures are available. Third, the volatility of these species is such that photoelectron spectra are readily obtainable, thus offering a direct experimental probe of their electronic structure which may serve as a check on the quality of the results of the calculations. Finally, cyclopentadienylmanganese tricarbonyl (**1**), which represents a convenient starting point for the investigation of this series, has recently been the subject of a detailed analysis by Fenske and Lichtenberger.[4]

## Experimental Section

**Photoelectron Spectra.** Cyclohexadienyl- (**2**),[5] cycloheptadienyl- (**3**),[6] and cycloheptatrienylmanganese tricarbonyl (**4**)[3] were prepared and isolated by reported methods. Photoelectron spectra were obtained on a Varian IEE-15 instrument operating in the uv configuration. All of the species **2**–**4** are solids and were introduced directly into the sample chamber, with mild heating (<50°) when necessary. Argon served as an internal standard and resolution check. The width at half-height of the argon peaks was better than 0.025 eV. The reported ionization potentials represent vertical transitions. The peak maxima for single ionizations were determined with an uncertainty of *ca.* ±0.05 eV. In instances where several ionizations are nearly degenerate, the maximum of the resulting band envelope is reported. In these instances the energies of the individual ionizations are less certain.

**Calculations.** Descriptions of the particular approximate molecular orbital method used here have appeared in the literature.[7,8] The only information required by this method is the geometry of the molecule and the atomic basis functions. The bond distances of the $Mn(CO)_3$ moiety were taken from the structure of $C_5H_5Mn(CO)_3$[9] and idealized to $C_{3v}$ symmetry. The geometry of the $Mn(CO)_3$ fragment is found to vary insignificantly from compound to compound and therefore was left the same for each calculation. This geometrical invariance allows the comparison of results through the series to be made more readily. The geometry for the $C_6H_7$ ligand was taken directly from the crystal structure of **2** as determined by Churchill and Scholer.[10] The structure of (azulene)$Mn_2(CO)_6$[11] was assumed to be a good model for the seven-membered ring in compounds **3** and **4**, after suitable minor bond length adjustments. Minor geometry changes do not significantly alter the conclusions of this study. The coordinates for these calculations are listed in Table I.

The calculations use a full atomic valence basis set, including the 1s function for hydrogen, the 2s and 2p functions for carbon and oxygen, and the 3d, 4s, and 4p functions for manganese. An exponent of 1.2 was used for the hydrogen 1s function. Basis functions for the carbon, oxygen, and manganese atoms are consistent with those used previously.[12] For the compounds included in this study there are between 58 and 70 calculated molecular orbitals, approximately half of which are occupied.

Appropriate basis set transformations were carried out in order to trace more clearly the principal interactions between the $Mn(CO)_3$[13] portion and the $\eta^5$ ligand. It was found that only the highest few occupied levels and the lowest few virtual levels have energies in the complex appreciably different from this calculated for the separated fragments. When the $3\sigma$ and $6\sigma$ levels of the carbonyl groups and the first three filled $\sigma$ levels and all the virtual $\sigma$ levels of the ligands were deleted from diagonalization of the Fock matrix, it was possible to save considerable time in the solution of the SCF equation with only negligible alteration of calculated eigenvalues and charge distributions.

## Results and Discussion

**Photoelectron Spectra.** The photoelectron spectra of compounds **2**–**4** are presented in Figure 1. The broad intense ionizations occurring with ionization potentials >12 eV represent transitions from the carbonyl $5\sigma$ and $1\pi$ orbitals as well as from certain of the ring $\sigma$ orbitals. The photoelectron spectra in this region are too complex to assign meaningfully, and no detailed analysis will be attempted. The well-resolved ionizations occurring between 7 and 12 eV, however, represent transitions from discrete occupied metal orbitals and from certain of the $\pi$ orbitals of the ring. The changes in these levels reflect changes in the electronic nature of the $\eta^5$ rings and in their interactions with the metal tricarbonyl portion. A more detailed assignment and interpretation of these ionizations is a principal aim of this paper.

**Calculations.** In order to trace clearly the bonding interactions in these complexes, it is convenient to perform a detailed preliminary analysis of the electronic structure of organic ligands independent of the perturbations introduced by the metal. This analysis, coupled with a calculation on the $Mn(CO)_3$ fragment,[14] allows changes in the bonding between metal and ligand through the series to be understood in terms

**Table I.** Atomic Coordinates (Å)

| | *x* | *y* | *z* |
|---|---|---|---|
| | | $Mn(CO)_3$ | |
| Mn | 0.0000 | 0.0000 | 0.0000 |
| C | 1.4951 | 0.0000 | −1.0023 |
| O | 2.4503 | 0.0000 | −1.6427 |
| C | −0.7476 | 1.2948 | −1.0023 |
| O | −1.2252 | 2.1221 | −1.6427 |
| C | −0.7476 | −1.2948 | −1.0023 |
| O | −1.2252 | −2.1221 | −1.6427 |
| | | $C_6H_7$ | |
| C1 | 0.9265 | 1.1920 | 1.6231 |
| C2 | −0.4578 | 1.2167 | 1.7244 |
| C3 | 1.1783 | 0.0000 | 1.7772 |
| C4 | −0.4578 | −1.2167 | 1.7244 |
| C5 | 0.9265 | −1.1920 | 1.6231 |
| C6 | 1.6531 | 0.0000 | 2.2067 |
| H1 | 1.2928 | 2.1757 | 1.5963 |
| H2 | −0.9569 | 2.1849 | 1.7610 |
| H3 | −2.2753 | 0.0000 | 1.8575 |
| H4 | −0.9569 | −2.1849 | 1.7610 |
| H5 | 1.2928 | −2.1757 | 1.5963 |
| H6 | 2.6552 | 0.0000 | 1.8931 |
| H7 | 1.6555 | 0.0000 | 2.9667 |
| | | $C_7H_9$ | |
| C1 | 1.0284 | 1.5100 | 1.4366 |
| C2 | −0.3372 | 1.2670 | 1.7204 |
| C3 | −0.9529 | 0.0000 | 1.8970 |
| C4 | −0.3372 | −1.2670 | 1.7204 |
| C5 | 1.0284 | −1.5100 | 1.4366 |
| H1 | 1.4159 | 2.4340 | 1.0074 |
| H2 | −0.9708 | 2.1492 | 1.8113 |
| H3 | −2.0069 | 0.0000 | 2.1747 |
| H4 | −0.9708 | −2.1492 | 1.8113 |
| H5 | 1.4159 | −2.4340 | 1.0074 |
| C6 | 2.2094 | −0.7400 | 1.8508 |
| C7 | 2.2094 | 0.7400 | 1.8508 |
| H6X | 2.4000 | −1.1030 | 2.8607 |
| H6N | 2.9891 | −1.1030 | 1.1811 |
| H7X | 2.4000 | 1.1030 | 2.8607 |
| H7N | 2.9891 | 1.1030 | 1.1811 |
| | | $C_7H_7$ | |
| C1 | 1.0284 | 1.4700 | 1.4366 |
| C2 | −0.3372 | 1.2670 | 1.7204 |
| C3 | −0.9529 | 0.0000 | 1.8970 |
| C4 | −0.3372 | −1.2670 | 1.7204 |
| C5 | 1.0284 | −1.4700 | 1.4366 |
| C6 | 2.1418 | −0.6820 | 2.0120 |
| C7 | 2.1418 | 0.6820 | 2.0120 |
| H1 | 1.4159 | 2.3940 | 1.0074 |
| H2 | −0.9708 | 2.1492 | 1.8113 |
| H3 | −2.0069 | 0.0000 | 2.1747 |
| H4 | −0.9703 | −2.1492 | 1.8113 |
| H5 | 1.4159 | −2.3940 | 1.0074 |
| H6 | 2.9901 | −1.3592 | 2.1112 |
| H7 | 2.9901 | 1.3592 | 2.1112 |

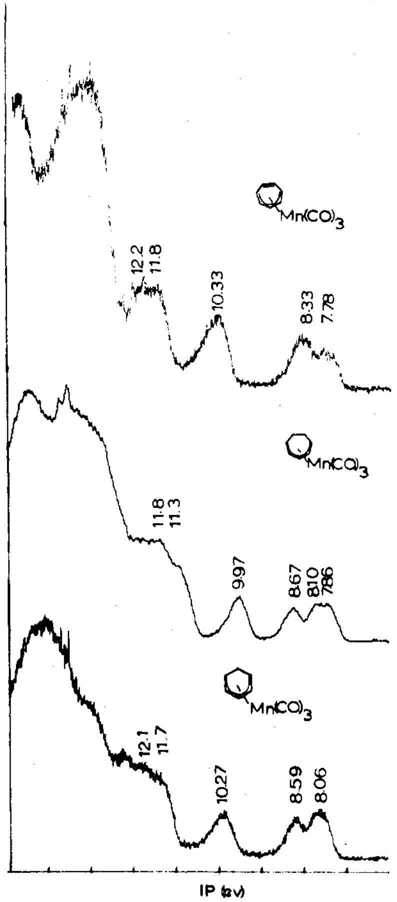

**Figure 1.** Photoelectron spectra of **2**, **3**, and **4**.

**Table II.** Calculated MO Energies (eV) for π Levels of Ligands[a]

| $C_5H_5^-$ | | $C_6H_7^-$ | | $C_7H_9^-$ | | $C_7H_7^-$ | |
|---|---|---|---|---|---|---|---|
| | | | Occupied | | | | |
| a$_2$'' | −9.01 | a'(a$_2$'') | −8.76 | a'(a$_2$'') | −8.83 | a'(a$_2$'') | −9.72 |
| | | | | | | a'(π) | −7.99 |
| e$_1$'' | −3.41 | a''(e$_1$'') | −5.59 | a''(e$_1$'') | −5.74 | a''(e$_1$'') | −6.54 |
| | | a'(e$_1$'') | −0.86 | a'(e$_1$'') | −0.97 | a'(e$_1$'') | +0.52 |
| | | | Virtual | | | | |
| e$_2$'' | +13.73 | a''(e$_2$'') | +7.39 | a''(e$_2$'') | +6.35 | a''(e$_2$'') | +2.78 |
| | | | | | | a''(π*) | +13.04 |
| | | a'(e$_2$'') | +16.02 | a'(e$_2$'') | +14.81 | a'(e$_2$'') | +14.56 |

[a] The MO's are identified by symmetry labels. The labels in parentheses identify the $C_5H_5^-$ orbitals from which the particular MO's derive. For $C_7H_7^-$ there are, in addition, the π and π* orbitals of the double bond.

of the interactions between the fragments. Thus, our study begins with calculations on each of the ligands,[14] the results of which are shown in Table II. Our attention will focus on the π orbitals of the ligand.

Qualitatively, the results in Table II may be understood if we first consider the symmetry orbitals of the $C_5H_5^-$ ring and then proceed in stages to the other ligands in the series. Under the $D_{5h}$ symmetry of the $C_5H_5^-$ ring, the carbon pπ orbitals combine to form the a$_2$'', e$_1$'', and e$_2$'' representations. In proceeding from $C_5H_5$ to $C_6H_7$, the reduction in symmetry produced by increasing the distance between two of the trigonal carbon atoms of the ligand causes a splitting of the e$_1$'' and e$_2$'' levels (Scheme I). The resulting ligands possess only mirror symmetry, and the resulting orbitals transform as a' and a''. For clarity in the following discussion, the symmetry labels of these orbitals will be followed in parentheses by the $C_5H_5^-$ orbitals from which they derive. The a'' levels so produced are antisymmetric with respect to reflection in the mirror plane bisecting the bond being broken. Therefore reduction of the 1,5 interaction stabilizes these levels. The opposite is true of the a' levels (a'(e$_1$'') and a'(e$_2$''); these levels are bonding across positions 1 and 5, and reduction of this interaction destabilizes them with respect to the e$_1$'' and e$_2$'' levels by a somewhat larger amount.

The introduction of the additional π and π* type orbitals in $C_7H_7$ results in a rather dramatic change in certain of the π levels (Scheme II). The π orbital is expected to be similar in energy to the a''(e$_1$'') orbital. The strong interaction between the bonding combination (π) of the double bond and a'(e$_1$'') leads to two new levels of a' symmetry. Here the orbitals in $C_7H_7$ are labeled according to the $C_5H_5^-$ orbital from which they were originally derived or with the label π or π*, depending on which fragment orbital makes the major contribution to the ligand orbital. The distinction is in this case

**Scheme I**

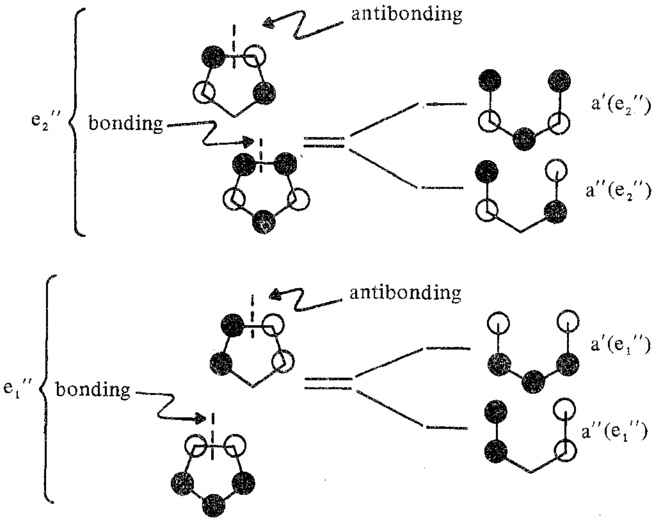

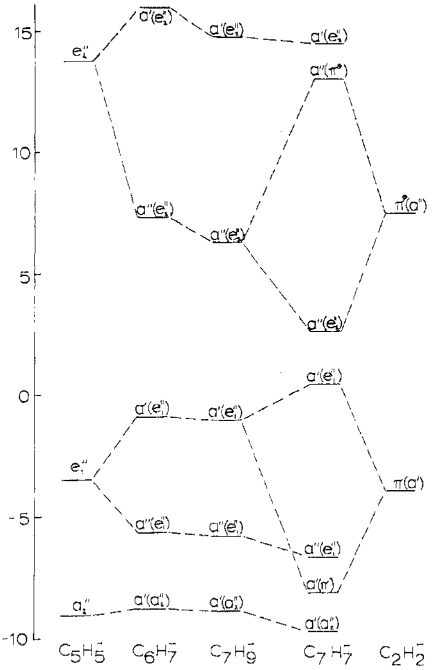

**Figure 2.** Correlation of calculated ligand eigenvalues for $C_5H_5^-$, $C_6H_7^-$, $C_7H_9^-$, and $C_7H_7^-$. Levels through a'(e$_1$'') are filled.

rather artificial, as all of these orbitals are highly delocalized over all seven carbon atoms. The $\pi^*$ orbital is expected to be close in energy to the a''(e2'') orbital. The bonding and antibonding combinations of $\pi^*$ with a''(e2'') similarly give rise to a''($\pi^*$) and a''(e2''). The symmetry-allowed interaction between $\pi^*$ and a''(e1'') is small because of the large energy separation between these two orbitals. The noteworthy aspects of the resulting energy levels are (a) the destabilization of the highest occupied MO a'(e1'') and (b) the introduction of a new virtual level a''(e2'') at a very low energy. This low-lying vacant MO may be of crucial importance in determining the fluxional character of $C_7H_7Mn(CO)_3$ (*vide infra*). Note that in the limit of regular geometry ($D_{7d}$) for the $C_7H_7$ group a'(e1'') and a''(e2'') become degenerate. These results are summarized in Figure 2.

Basis set transformations were carried out in terms of the eigenfunctions of the $Mn(CO)_3^+$ fragment as well as those of the ligand. The $M(CO)_3$ unit is extremely common in transition metal organometallic chemistry and has been the subject of other discussions.[13] The nature of the metal to carbonyl bond has also received much attention.[12] Because our primary interest is in the metal–olefin interaction, we will focus our attention on how the carbonyl groups affect the metal orbitals available for bonding to the ring. We have found the coordinate system in Table I most convenient for this purpose. In this coordinate system, the metal is placed at the origin and the carbonyl groups are symmetrically positioned about the 3 axis. The ring is approximately centered about the positive 3 axis in a plane roughly parallel to the *xy* plane.

**Scheme II**

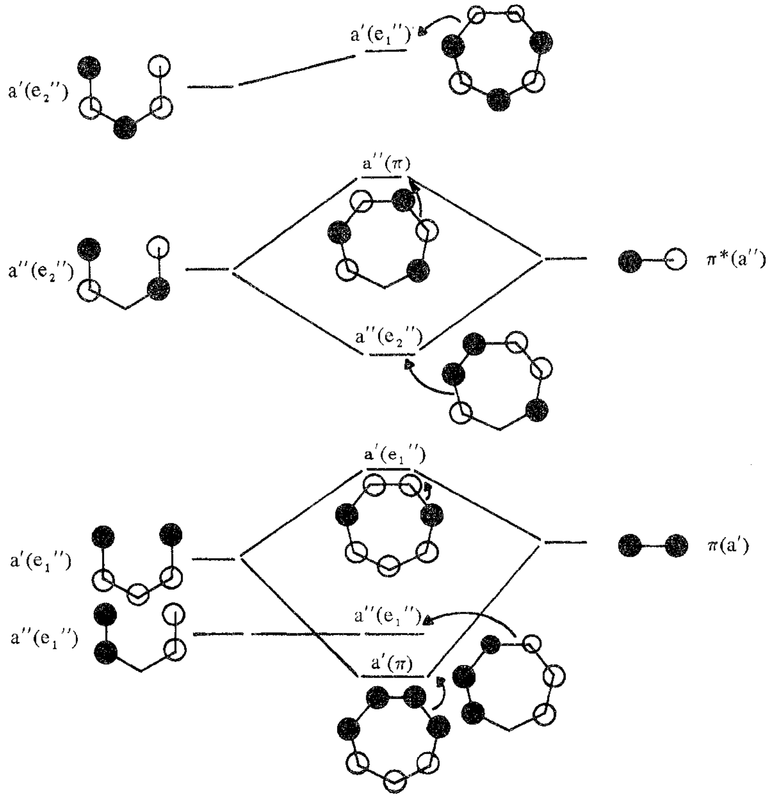

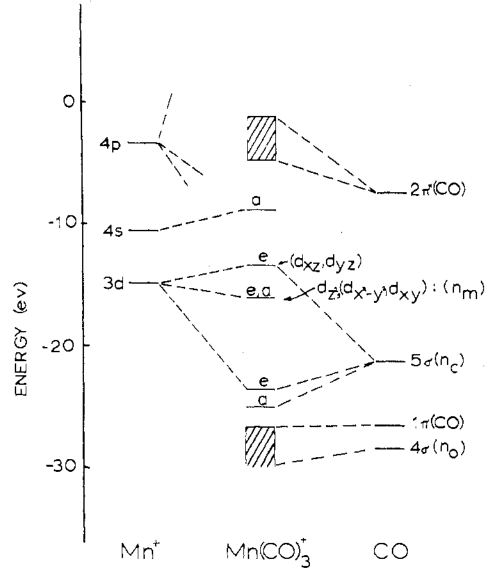

**Figure 3.** Molecular orbital interaction diagram for $Mn(CO)_3^+$. Levels through $n_m$ are filled.

Consider first the interaction of the carbonyl 5σ with the metal d orbitals. In this coordinate system the 5σ orbitals interact primarily with the metal ($d_{xz}$, $d_{yz}$) orbitals. The bonding combinations represent σ donation from the carbonyl groups to the metal. The antibonding combination is primarily ($d_{xz}$, $d_{yz}$) in character. This level is virtual and is of the correct symmetry to act as a π acceptor from the $\eta^5$ ring.

The π* orbitals of the carbonyls are available for back-donation from the metal. In this coordinate system the carbonyl π* orbitals interact primarily with the metal $d_{z^2}$ and ($d_{x^2-y^2}$, $d_{xy}$) orbitals, which under $C_{3v}$ symmetry correspond to the occupied a and e combinations, respectively. These levels are split only slightly.

In the following discussion, the $Mn(CO)_3$ orbitals will be referred to according to their primary metal character. Thus the highest occupied molecular orbitals, or HOMO's, are the metal ($d_{x^2-y^2}$, $d_{xy}$) and $d_{z^2}$ orbitals ($n_m$) and the lowest unoccupied molecular orbitals, or LUMO's, are the metal $d_{xz}$ and $d_{yz}$ orbitals. These results are summarized in Figure 3.

**Metal-Ligand Bonding.** Having described the structure of the $\eta^5$ ligands and of the $Mn(CO)_3$ group, we now consider the interactions between these fragments. Qualitative features of the pentadienyl ligand to metal bond have been discussed previously.[15] The results of the calculations in terms of the eigenvalues and principal contributions to the orbitals are illustrated for **3** and **4** in the molecular orbital diagram of Figure 4.

First, after correcting the energies of the fragment orbitals for charge effects, most of the orbitals transfer from the fragment to the molecule with little change in character or eigenvalue, thus confirming the interpretive value of considering the metal and ligand separately. For reasons of overlap, the principal interaction between the ring and the metal may be expected to arise from those orbitals on the ring which are of the correct symmetry to interact with the metal $d_{xz}$ and $d_{yz}$ orbitals. As the MO diagrams indicate, this interaction is also favored energetically. Thus for $C_7H_9$, the interaction of the $d_{xz}$ orbital with a'($e_1''$) stabilizes this ligand level below the occupied metal levels. The interaction of a''($e_1''$) with $d_{yz}$ is also favored by overlap, but because of the greater energy separation, the interaction is relatively less important. The a'($e_1''$) and a''($e_1''$) orbitals are the HOMO's of the ring, and the $d_{xz}$ and $d_{yz}$ orbitals are the LUMO's of the metal. Therefore, interaction between these orbitals results in electron donation from the ring to the metal.

Back-donation from the metal to the ring is found to be relatively less important. For $C_7H_9$, the overlap of the $Mn(CO)_3$ ($d_{x^2-y^2}$, $d_{xy}$) orbitals with a''($e_2''$) and a'($e_2''$) is small and the separation of orbital energies is relatively great. Also, the overlap of the metal $d_{z^2}$ orbital with the symmetric ring π orbital a'($a_2''$) is small because the lower lobes of the π orbitals lie on or near the nodal cone of $d_{z^2}$. Therefore, these metal orbitals are expected to be altered to a lesser extent by interaction with the π ligand. These comments for the orbitals of $C_7H_9Mn(CO)_3$ apply equally to the corresponding orbitals in $C_6H_7Mn(CO)_3$ and $C_7H_7Mn(CO)_3$.

The interactions in $C_7H_7Mn(CO)_3$ require further consideration. As mentioned earlier in the discussion of the free

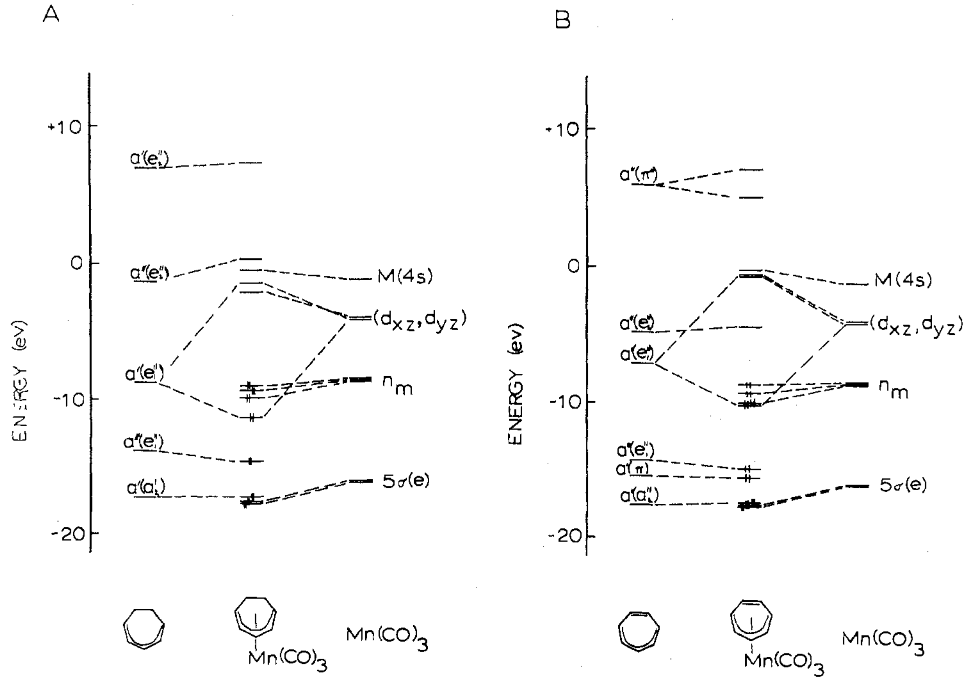

**Figure 4.** Molecular orbital interaction diagrams for (A) $C_7H_9Mn(CO)_3$ and (B) $C_7H_7Mn(CO)_3$. Fragment levels are shown corrected for the effects of charge transfer.

**Table III.** Observed IP's and Calculated MO Energies

| $CpMn(CO)_3$ | | | **2** | | | **3** | | | **4** | | |
|---|---|---|---|---|---|---|---|---|---|---|---|
| $IP_{obsd}$,[a] eV | $E_{calcd}$,[b] eV | Type[c] | $IP_{obsd}$, eV | $E_{calcd}$, eV | Type | $IP_{obsd}$, eV | $E_{calcd}$, eV | Type | $IP_{obsd}$, eV | $E_{calcd}$, eV | Type |
| 8.0–8.5 | −9.35 | $n_m$ | 8.06 | −9.05 | $n_m$ | 7.86 | −8.83 | $n_m$ | 7.66 | −8.72 | $n_m$ |
| | −9.35 | $n_m$ | | −9.19 | $n_m$ | 8.10 | −9.19 | $n_m$ | 7.86 | −9.31 | $n_m$ |
| | −9.48 | $n_m$ | | −9.68 | $n_m$ | | −9.69 | $n_m$ | 8.33 | −10.06 | $n_m$ |
| 10 | −13.53 | $\pi_1{}^b$ | −8.59 | −11.68 | $\pi_1{}^b$ | −8.67 | −11.21 | $\pi_1{}^b$ | | −10.20 | $\pi_1{}^b$ |
| | −13.57 | $\pi_1{}^b$ | −10.25 | −14.94 | $\pi_1{}^b$ | −9.97 | −14.43 | $\pi_1{}^b$ | 10.33 | −15.01 | $\pi_1{}^b$ |
| | | | | | | | | | | −15.7 | $\pi_1$ |

[a] Observed ionization potential. [b] Calculated eigenvalue. [c] Type of ionization: $n_m$, nonbonding metal orbital; $\pi_1{}^b$, metal–ligand bonding orbital; $\pi_1$, $\pi$ ligand orbital.

ligand, the $\pi$ orbital (of a' symmetry) is similar in energy to the a''($e_1''$) orbital but interacts strongly only with a'($e_1''$), resulting in two new levels delocalized over the $C_7H_7$ ring. The $\pi$ orbital overlaps poorly with the metal orbitals and therefore does not have an appreciable influence on the metal–ligand bond directly. The effect of this orbital should therefore be indirect, by way of its interaction with the bonding levels of the $C_5H_5$ portion of the ring.

In fact, the destabilization of the a'($e_1''$) orbital results in a more favorable interaction with the $d_{xz}$ $Mn(CO)_3$ orbital. Correspondingly, the low-lying virtual level a''($e_2''$) produced by the interaction of $\pi^*$ with a''($e_2''$) of the $C_5H_5$ unit is closer to the occupied metal levels and therefore is a better charge acceptor. Overall, the total charge is calculated to be equally well compensated in **2**, **3**, and **4**, but the total interaction is stronger in **4** relative to its nonconjugated analogs **2** and **3**.

The existence of the low-lying a''($e_2''$) orbital is perhaps significant in another context as well. Pearson[16] has stated that the presence of a low-lying orbital of the correct symmetry may produce low-energy pathways for geometrical distortion. It seems likely that this LUMO is important in determining pathways by which $C_7H_7Mn(CO)_3$ may undergo its degenerate rearrangement. This possibility is being further explored in connection with other ring whizzers, and a detailed discussion will be published separately.

**Assignment of Photoelectron Spectra.** The calculated eigenvalues for **2**–**4** and $CpMn(CO)_3$ are correlated in Figure 5. The trends in these eigenvalues allow the following assignment of the observed PE spectra. For $C_6H_7Mn(CO)_3$, the overlapping ionizations around 8.06 eV are associated with levels primarily metal in character. The ionization occurring at 8.59 eV is associated with the orbital resulting from the bonding interaction between the ring a'($e_1''$) and the metal $d_{xz}$ orbital. The ionization at 10.27 eV represents the ring a''($e_1''$). Higher ionization potentials represent the deeper $\sigma$ and $\pi$ orbitals. The ionizations of $C_7H_9Mn(CO)_3$ are similar. Ionizations associated with metal levels occur between 7.86 and 8.10 eV. The a'($e_1''$) and a''($e_1''$) ionizations occur at 8.67 and 9.97 eV, respectively.

For $C_7H_7Mn(CO)_3$, ionizations associated with the metal levels occur around 7.78 eV. The ionizations of the metal levels for all three compounds are at nearly the same energy, as was predicted from the theoretical analysis. The a'($e_1''$) ionization is at 8.33 eV for this molecule, which represents a significant destabilization of this ionization over that in molecules **3** and **4**, as predicted. The stabilized $\pi$ level of the ring and the a''($e_1''$) level are both assigned to the peak at 10.33 eV. The ionization potentials for these two levels are expected to be similar, and the observed near degeneracy is consistent with the increased relative amplitude and half-width of this band as compared to the a''($e_1''$) bands of $C_6H_7Mn(CO)_3$ and $C_7H_9Mn(CO)_3$.

Table III shows the observed IP's together with the calculated energy of the MO with which the ionization is associated. The eigenvalues of a ground-state Hartree–Fock calculation are not expected to coincide exactly with experimental ionization potentials because the calculation neglects electron correlation and electron relaxation in the excited ion.[17] Our eigenvalues, which are the results of approximate methods, are uniformly too large in magnitude, as has also often been observed for *ab initio* calculations.

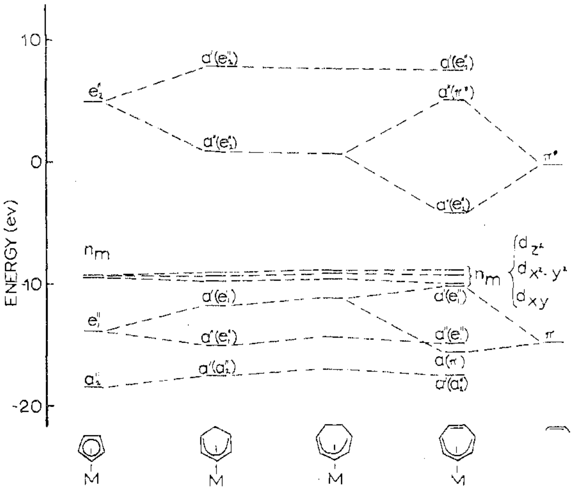

**Figure 5.** Correlation of calculated eigenvalues for $CpMn(CO)_3$, **2**, **3**, and **4**. Levels through $n_m$ are filled.

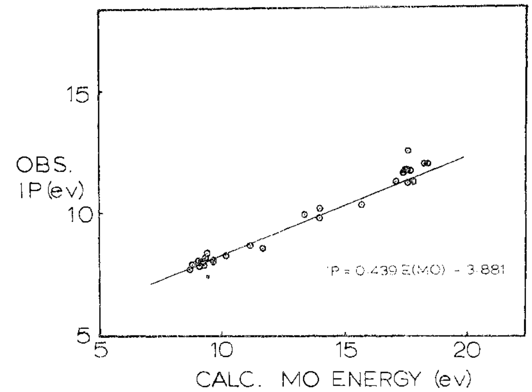

**Figure 6.** Plot of the observed ionization potentials of $CpMn(CO)_3$, **2**, **3**, and **4** *vs.* the assigned calculated MO energy.

Recently there has been some question concerning the validity of using Koopman's theorem for the comparison of both metal and ligand eigenvalues with ionization potentials.[18] We note here, however, that a consistent assignment of the ionization potentials is accomplished without reversing the ordering of any of the calculated levels. A plot of observed IP's against calculated MO energies is shown in Figure 6. The observed IP's are seen to be related to the calculated MO eigenvalues quite accurately by a linear relationship (correlation coefficient 0.99)

$$\text{predicted IP} = -0.4393E_{calcd} + 3.881$$

Note that both the metal and the ring levels are well repre-

**Table IV.** Correlation of Calculated MO Energies with Observed Ionization Potentials for $C_7H_7Mn(CO)_3$

| Calcd MO energy, eV | Predicted IP, eV | Obsd IP, eV | Type |
|---|---|---|---|
| −8.72 | −7.71 | −7.7 | M |
| −9.31 | −7.97 | −7.9 | M |
| −10.06 | −8.30 | −8.3 | M |
| −10.20 | −8.36 | | $\pi$ |
| −15.01 | −10.47 | −10.3 | $\pi$ |
| −15.67 | −10.76 | | $\pi$ |
| −17.47 | −11.45 | $\sim-11.8$ | $\pi$ |
| −17.58 | −11.60 | | CO |
| −17.70 | −11.65 | | $\sigma$ |

sented by the same line for these molecules. The agreement between calculated and observed values for $C_7H_7Mn(CO)_3$ is shown in Table IV. The agreement is considered quite satisfactory, since the experimental values are estimated to be uncertain by about 0.1 eV. Thus we feel that violations of Koopman's theorem are sufficiently close to constant in the series to allow PES to be useful as a probe of electronic structure. The consistent explanation of the spectra allowed by our calculations indicates that they adequately account for the principal interactions and thus allow a more detailed understanding of the bonding in these molecules.

**Acknowledgment.** The authors are grateful to the National Science Foundation (Grant GP 16358) and to the Research Committee of the University of Wisconsin for generous financial support. We further wish to thank Professor Richard Fenske for his interest in this problem and for the use of his program. D. L. L. also acknowledges an NDEA-IV Fellowship (Grant 69-03546.1).

**Registry No.** $CpMn(CO)_3$, 12079-65-1; **2**, 12108-14-4; **3**, 32798-86-0; **4**, 53011-14-6; $C_5H_5^-$, 12127-83-2; $C_6H_7^-$, 27900-34-1; $C_7H_9^-$, 26810-99-1; $C_7H_7^-$, 29875-65-8.

## References and Notes

(1) For leading references see F. A. Cotton, *Accounts Chem. Res.*, **1**, 257 (1968).

(2) (a) T. A. Manuel and F. G. A. Stone, *Proc. Chem. Soc., London*, 90 (1959); *J. Amer. Chem. Soc.*, **82**, 366 (1960); (b) M. D. Rausch and G. N. Schrauzer, *Chem. Ind. (London)*, 957 (1959); (c) A. Nakamura and N. Hagihara, *Bull. Chem. Soc. Jap.*, **32**, 880 (1959).

(3) T. H. Whitesides and R. A. Budnik, *Chem. Commun.*, 1514 (1971).

(4) D. L. Lichtenberger and R. F. Fenske, private communication.

(5) G. Winkhaus, L. Pratt, and G. Wilkinson, *J. Chem. Soc.*, 3807 (1961).

(6) F. Hague, J. Miller, P. L. Pauson, and J. B. P. Tripathi, *J. Chem. Soc. C*, 743 (1971).

(7) R. F. Fenske, *Pure Appl. Chem.*, **27**, 61 (1971).

(8) R. F. Fenske and M. B. Hall, *Inorg. Chem.*, **11**, 768 (1972).

(9) A. F. Berndt and R. E. Marsh, *Acta Crystallogr.*, **16**, 118 (1963).

(10) M. R. Churchill and F. R. Scholer, *Inorg. Chem.*, **8**, 1950 (1969).

(11) M. R. Churchill and P. H. Bird, *Inorg. Chem.*, **7**, 1793 (1968).

(12) M. B. Hall and R. F. Fenske, *Inorg. Chem.*, **11**, 1619 (1972).

(13) S. F. A. Kettle, *Inorg. Chem.*, **4**, 1661 (1965).

(14) The ligands were calculated as anions and $Mn(CO)_3$ was calculated as a cation to avoid open-shell configurations.

(15) L. E. Orgel, *J. Inorg. Nucl. Chem.*, **2**, 315 (1956).

(16) R. G. Pearson, *Theor. Chim. Acta*, **16**, 107 (1970).

(17) W. G. Richards, *Int. J. Mass. Spectrom. Ion Phys.*, **2**, 419 (1969).

(18) (a) M. Rohmer and A. Veillard, *J. Chem. Soc., Chem. Commun.*, 7, 250 (1973); (b) M. Coutiere, J. Demuynck, and A. Veillard, *Theor. Chim. Acta*, **27**, 281 (1972).

---

Contribution from the Department of Chemistry,
University of Alberta, Edmonton, Alberta T6G-2E1

# Synthesis and Characterization of Dithiolene Complexes of the Early Transition Metals

JOEL L. MARTIN and JOSEF TAKATS*

*Received May 14, 1974* AIC40307L

The synthesis of tris(dithiolene) complexes of the type $[R_4E]_xM(S_2C_6H_3Y)_3$ (where $R_4E$ is a tetraphenylarsonium or tetraalkylammonium ion; M is Ti, Zr, or Hf and $x = 2$ or M is Ta or Nb and $x = 1$; and Y is H or $CH_3$) has been accomplished by reaction of the appropriate metal amide with a mixture of the dithiol and its sodium salt in THF. The results of ir, visible, and uv spectra, conductivity, $^1$H and limited $^{13}$C nmr studies are presented. The electronic spectra are dominated by ligand-to-metal charge-transfer bands. The band positions change in the expected order Ti < Zr $\sim$ Hf, Nb < Ta, Nb < Zr, and Ta < Hf. The variety of coordination geometries within the reported complexes is noted and the importance of matching ligand and metal d orbital energies for the stabilization of trigonal prismatic geometry is discussed.

The chemistry of 1,2-dithiolene complexes of the transition metals has been the subject of considerable study over the past decade.[1-7] It is noteworthy, however, that during this period of great activity, few complexes of the early transition metals[8-10] have been reported aside from those of vanadium. The inability to synthesize these complexes can be traced to the lack of a suitable preparative method. Indeed, attempts to obtain dithiolene complexes of the early transition metals by known synthetic procedures, *e.g.*, the reaction of anhydrous metal chlorides with dithiols or their sodium salts, have invariably led to failures except in the cases noted above, both in our laboratories and elsewhere.[9] It seemed to us that the difficulties presented by the known methods could be overcome by using starting materials with more readily displaceable ligands. In this context, the extensive investigations of Bradley,[11,12] Thomas,[13] and Lappert[14] into the reactivity of transition metal amido derivatives, $M(NR_2)_x$, seemed particularly relevant. Indeed, these authors have amply demonstrated the usefulness of these complexes both in insertion reactions and in reactions with protic ligands. However, the reaction of these metal amides with 1,2-dithiols seems to have been overlooked.

In this article, we report the detailed synthesis of benzene-1,2-dithiol and toluene-3,4-dithiol complexes of Ti, Zr, Hf, Nb, and Ta utilizing the corresponding metal amides as starting materials. Further, we discuss the results of physical studies carried out on these complexes. Comparison of our results with previous investigations has clarified several trends and greatly assisted our understanding of the behavior of dithiolene complexes.

## Experimental Section

All operations were performed in Schlenk type apparatus under an atmosphere of nitrogen dried by passing through a column of